

An Extension of Quasi Linkage Equilibrium

Kai S. Shimagaki^{1,2,†}, Jorge Fernandez-de-Cossio-Diaz³, Mauro Pastore⁴, Rémi Monasson^{5,6,7}, Simona Cocco^{5,6,7}, and John P. Barton^{1,2,†}

¹Department of Computational and Systems Biology, University of Pittsburgh School of Medicine, USA.

²Department of Physics and Astronomy, University of Pittsburgh, USA.

³Institut de Physique Théorique, Université Paris-Saclay, CNRS, CEA, Gif-sur-Yvette, France.

⁴The Abdus Salam International Centre for Theoretical Physics (ICTP), Strada Costiera 11, 34151 Trieste, Italy

⁵Laboratoire de Physique de École Normale Supérieure, France

⁶PSL & CNRS UMR 8023, France

⁷Sorbonne Université, 75005 Paris, France

†Address correspondence to: kais@pitt.edu (K.S.S), jpbarton@pitt.edu (J.P.B.).

A central question in evolutionary biology is how to quantitatively understand the dynamics of genetically diverse populations. Modeling the genotype distribution is challenging, as it ultimately requires tracking all correlations (or cumulants) among alleles at different loci. The quasi-linkage equilibrium (QLE) approximation simplifies this by assuming that correlations between alleles at different loci are weak – i.e., low linkage disequilibrium – allowing their dynamics to be modeled perturbatively. However, QLE breaks down under strong selection, weak recombination, or significant epistatic interactions. We extend the multilocus QLE framework to allow cumulants up to order K to evolve dynamically, while higher-order cumulants ($> K$) are assumed to equilibrate rapidly. This extended QLE (exQLE) framework yields a general equation of motion for cumulants up to order K , which parallels the standard QLE dynamics (recovered when $K = 1$). In this formulation, cumulant dynamics are driven by the gradient of average fitness, mediated by a geometrically interpretable matrix that stems from competition among genotypes. Our analysis shows that the exQLE with $K = 2$ accurately captures cumulant dynamics even when the fitness function includes higher-order (e.g., third- or fourth-order) epistatic interactions, capabilities that standard QLE lacks. We also applied the exQLE framework to infer fitness parameters from temporal sequence data. Overall, exQLE provides a systematic and interpretable approximation scheme, leveraging analytical cumulant dynamics and reducing complexity by progressively truncating higher-order cumulants.

Introduction

One of the central questions in evolutionary biology is to understand how populations evolve under natural selection and other evolutionary forces^{1–4}. The aim is to model the dynamics of genotype distribution over time. A major challenge arises from the non-random association of alleles (e.g., nucleotides) at different loci (positions in a linear sequence), known as linkage disequilibrium (LD)⁵. In the absence of LD, a state known as linkage equilibrium, each allele evolves independently and its dynamics can be solved exactly¹. However, this condition is overly restrictive. Indeed, natural selection can induce LD, which causes the dynamics of different alleles to become correlated. A general description of population evolution requires accounting for an exponentially increasing number of allele combinations across loci, which are coupled through LD^{4,6}.

Quasi-linkage equilibrium (QLE) is a state where LD is

present but small, the rate of changes in LD is faster than those in individual allele frequencies, thereby LD rapidly converges to equilibria^{4,7}. In contrast to linkage equilibrium, QLE can naturally occur under conditions of weak selection and/or weak epistasis, coupled with high recombination rates. This results in distinct time scales: the slow dynamics of individual allele frequency, governed by selection (with a time scale of $1/s$, where s is the selection strength), and the rapid decay of linkage disequilibrium (with a time scale of $1/r$, where r is the recombination rate). The slow dynamics are driven by gradients of average fitness with respect to cumulants^{7–10}. Practically, QLE serves as a useful platform to investigate the collective evolution of alleles in multilocus systems, as it simplifies the mathematical structure, and reduces the dimensionality of genotype distribution¹⁰.

QLE has primarily been examined within a two-locus, two-allele framework, initially proposed by Kimura⁷ and further investigated by Nagylaki, Barton and colleagues^{11,12}. Barton and Turelli developed a framework for describing evolution in centered moments^{13,14}, encompassing second and higher orders under arbitrary selection and recombination, which was later generalized by Kirkpatrick et al.¹⁵. Nagylaki et al. also focused on the evolution of multilocus systems, rigorously examining the sufficient conditions for convergence to equilibria or QLE manifolds using a small-epistasis perturbation theory^{16,17}. Recently, Neher and Shraiman further developed the QLE theory for multilocus systems, building on the foundational work by Barton and Turelli^{13,14}. This has made the QLE theory more conceptually and analytically streamlined¹⁰, elucidating that the cumulant dynamics are driven by the gradient of average fitness. Recent work leveraged the analytically tractable QLE’s cumulant dynamics to infer fitness parameters, an important challenge in evolutionary biology^{18,19}.

Strong selection can at least transiently break down QLE. During a selective sweep, linked loci can exhibit positive LD as the selected loci drag other linked loci, known as genetic hitchhiking²⁰ (see ref.²¹ for a broader discussion). In contrast, negative LD may arise between selected loci, known as the Hill-Robertson interference effect²² (see also ref.²³). These dynamics violate QLE, but equilibrium may re-establish after the sweep concludes. However, epistatic interactions between different loci can permanently violate the QLE assumptions^{8,17}. For example, if pairs of loci are

selected due to epistatic interactions, then the pairwise LD or pairwise cumulants of alleles at different loci cannot relax to equilibria rapidly. As a result, the decay times of the pairwise cumulants become comparable to the timescales of individual allele frequencies.

Theoretical and computational studies offer insights into how epistasis arises^{24,25}, the structure of epistasis^{26–29}, and how epistasis influences evolutionary dynamics^{30,31} (See also recent reviews^{32,33}). However, it remains challenging to understand how populations evolve in the presence of higher-order epistasis. Recent studies have revealed the prevalence and complex patterns of epistasis^{34–40}, including the presence of hierarchical higher-order epistasis in various contexts^{41–48}. This underscores the need to extend QLE theory to accommodate a prevalent and broader range of epistasis.

Here, we propose an extended QLE (exQLE) framework that relaxes the assumptions that while individual allele frequencies evolve slowly, second and higher-order cumulants are small and converge rapidly to equilibria. Instead, we allow cumulants up to an arbitrary order K to evolve dynamically while assuming those of order $K + 1$ and above remain small and rapidly reach equilibrium. We first derived a general expression for cumulant dynamics under an arbitrary order of cumulants and genotype distributions, showing that their evolution is driven by the gradient of the average fitness function with respect to the cumulants. This forms the basis of the exQLE formulation, allowing for systematic relaxation of the assumption that cumulants above the $K = 1$ order are effectively in steady state.

As an example, we analyze the $K = 2$ case, which is the simplest extension of QLE, demonstrating the dynamics of first- and second-order cumulants. These expressions describe how fitness parameters influence the cumulant dynamics and can be used to infer these fitness parameters. Interestingly, the expressions for the cumulant dynamics from exQLE match exactly with those derived by projecting genotype dynamics onto the space of cumulants in the diffusion approximation of the Wright-Fisher (WF) process^{49,50}. Furthermore, the exQLE framework, whose cumulant dynamics are fully characterized by combinations of cumulants, readily provides a systematic approach to approximate the dynamics by progressively reducing cumulants in an order-by-order manner. This systematic approach reproduces the previously reported QLE-based epistasis inference method with a Gaussian closure (GC) scheme⁵¹, along with alternative inference methods.

Evolution of genetic traits and Quasi-Linkage Equilibrium theory

Here, we consider the evolution of a population of individuals, described by a probability distribution of genotypes, $P(\mathbf{g}, t)$ with a binary genotype $\mathbf{g} \in \{-1, +1\}^L$ of length L . The average of an arbitrary genetic trait across a temporal genetic distribution is defined as $\langle G \rangle := \sum_{\mathbf{g}} P(\mathbf{g}, t)G(\mathbf{g})$. For the sake of simplicity, the time dependency (t) has been omitted. The principle governing population evolution is that fitter genotypes produce more offspring, lead-

ing to their increased frequency in the next generation. Let $F(\mathbf{g})$ denotes a fitness function, mapping genotypes to Malthusian fitness^{52,53}, then the genotype dynamics can then be expressed as $P(\mathbf{g}, t + \Delta t) = \frac{e^{\Delta t F(\mathbf{g})}}{\langle e^{\Delta t F(\mathbf{g})} \rangle} P(\mathbf{g}, t)$ over a time period Δt . When the selection is small such that $|\log(e^{\Delta t F}/\langle e^{\Delta t F} \rangle)| \ll 1$, the expected genotype follows $P(\mathbf{g}, t + \Delta t) \simeq P(\mathbf{g}, t) + \Delta t[F(\mathbf{g}) - \langle F \rangle]P(\mathbf{g}, t)$. Considering mutation and recombination effects, which operate on individuals and introduce genetic variation, the dynamics of the genotype distribution is described by the following master equation:

$$\begin{aligned} \dot{P}(\mathbf{g}, t) &= [F(\mathbf{g}) - \langle F \rangle] P(\mathbf{g}, t) \\ &+ \mu \sum_{\mathbf{g}' : d(\mathbf{g}, \mathbf{g}')=1} [P(\mathbf{g}', t) - P(\mathbf{g}, t)] \\ &+ r \sum_{\mathbf{g}', \mathbf{g}''} R(\mathbf{g} | \mathbf{g}', \mathbf{g}'') P(\mathbf{g}', t) P(\mathbf{g}'', t) - r P(\mathbf{g}, t) \end{aligned} \quad (1)$$

where μ , r are, respectively, mutation and recombination rates, $d(\mathbf{g}, \mathbf{g}')$ represents the Hamming distance, and $R(\mathbf{g} | \mathbf{g}', \mathbf{g}'')$ is the probability that genotypes \mathbf{g}' and \mathbf{g}'' produce genotype \mathbf{g} through recombination.

For simplicity, we temporarily ignore the contributions of mutation and recombination ($\mu = 0$ and $r = 0$), as their effects do not alter the following discussion and are explicitly detailed in refs.^{10,50}. Given this dynamical rule, the equation of motion for the average arbitrary trait or arbitrary function of \mathbf{g} denoted as G , is given as:

$$\frac{d}{dt} \langle G \rangle = \text{Cov}(F, G) \quad (2)$$

which is known as Price's equation⁵⁴ or “second theorem” of natural selection⁵⁵, and can be viewed as a generalization of Fisher's “fundamental theorem”^{2,54}. Throughout this paper, we assume the fitness function is expressed as

$$F(\mathbf{g}) = \sum_i s_i g_i + \sum_{i < j} s_{ij} g_i g_j + \dots, \quad (3)$$

where s_i and s_{ij} are time-independent coefficients characterizing the effects of a single mutation at site i (selection coefficient) and a double mutation at site i and j (pairwise epistatic coefficient). To describe dynamics of cumulants below, we define the following cumulant generating function under an arbitrary genotype distribution, $P(\mathbf{g}, t)$, parameterized by $\phi = (\phi_1, \dots, \phi_L)^\top$, given as:

$$\Phi(\phi, t) := \log \left(\sum_{\mathbf{g}} P(\mathbf{g}, t) e^{\phi^\top \mathbf{g}} \right). \quad (4)$$

For notational convenience, we define $\chi_i^\phi := \partial_{\phi_i} \Phi$, $\chi_{ij}^\phi := \partial_{\phi_i} \partial_{\phi_j} \Phi$, and subsequent orders, which results in the cumulants, $\chi_i = \chi_i^\phi|_{\phi=0}$, $\chi_{ij} = \chi_{ij}^\phi|_{\phi=0}$, respectively. Additionally, we define $\langle G \rangle_\phi := \sum_{\mathbf{g}} G(\mathbf{g}) P(\mathbf{g}, t) e^{\phi^\top \mathbf{g}} / \sum_{\mathbf{g}} P(\mathbf{g}, t) e^{\phi^\top \mathbf{g}}$, which yields $\langle G \rangle_{\phi=0} = \langle G \rangle$. Based on Price's equation Eq. (2)

and Eq. (4), along with the assumption that $P(g, t)$ does not induce strong interactions between sites and that the dynamics of higher-order cumulants are negligibly small, it is derived that the dynamics of first-order cumulants as $\dot{\chi}_i \simeq \sum_j \chi_{ij} \partial_{\chi_j} \langle F \rangle$ (ref.⁹) The dynamics of arbitrary traits were expressed as a linear combination of first-order cumulant dynamics, $\frac{d\langle G \rangle}{dt} = \sum_i \dot{\chi}_i \partial_{\chi_i} \langle G \rangle$. In the QLE framework, we assume that higher-order cumulants change faster than first-order cumulants, allowing the former to quickly reach equilibrium while the latter are still evolving ($\dot{\chi}_{ij} = \dot{\chi}_{ijk} = \dots = 0$).

Extension of QLE theory

We begin by expressing the equation of motion for cumulants under any arbitrary genotype distribution. We then consider a scenario where the K -th order cumulants evolve dynamically, while higher-order cumulants (those of order $K + 1$ and above) remain small and rapidly reach equilibria.

To express the general form of cumulant dynamics, let $\mathcal{I}, \mathcal{J}, \mathcal{K}$ denote multi-indices over loci, e.g., $\mathcal{I} = (i_1, i_2, \dots)$ where i_1, i_2, \dots are indices of loci. Using the cumulant generating function and the relation $\partial_t \Phi(\phi, t) = \langle F \rangle_\phi - \langle F \rangle$, the dynamics of cumulants of arbitrary order can be expressed as

$$\begin{aligned}\dot{\chi}_{\mathcal{I}} &= \partial_t \partial_{\phi_{\mathcal{I}}} \Phi(\phi, t)|_{\phi=0} \\ &= \partial_{\phi_{\mathcal{I}}} \langle F \rangle_\phi|_{\phi=0}.\end{aligned}\quad (5)$$

By denoting moments $\mu_{\mathcal{I}}^\phi := e^{-\Phi} \partial_{\phi_{\mathcal{I}}} e^\Phi$ with $\mu_{\mathcal{I}} = \mu_{\mathcal{I}}^\phi|_{\phi=0}$, the last expression can be further written as:

$$\begin{aligned}\partial_{\phi_{\mathcal{I}}} \langle F \rangle_\phi|_{\phi=0} &= \sum_{\mathcal{K}} \frac{\partial \langle F \rangle}{\partial \mu_{\mathcal{K}}} \left. \frac{\partial \mu_{\mathcal{K}}^\phi}{\partial \phi_{\mathcal{I}}} \right|_{\phi=0} \\ &= \sum_{\mathcal{J}, \mathcal{K}} \frac{\partial \langle F \rangle}{\partial \chi_{\mathcal{J}}} \left. \frac{\partial \chi_{\mathcal{J}}}{\partial \mu_{\mathcal{K}}} \frac{\partial \mu_{\mathcal{K}}^\phi}{\partial \phi_{\mathcal{I}}} \right|_{\phi=0}.\end{aligned}\quad (6)$$

In the first equality, we use the fact that $\frac{\partial \langle F \rangle}{\partial \mu_L}$ is independent of the statistical variables. From the first to the second line, we convert from moment-based to cumulant-based expressions.

Therefore, by denoting χ and ∇_{χ} as $\chi := ((\chi_i)_i, (\chi_{ij})_{i < j}, \dots)$ and $\nabla_{\chi} := ((\partial_{\chi_i})_i, (\partial_{\chi_{ij}})_{i < j}, \dots)$, the cumulant dynamics can be generally expressed as:

$$\begin{aligned}\dot{\chi} &= D(\chi) \nabla_{\chi} \langle F \rangle \\ D_{\mathcal{I}, \mathcal{J}} &:= \sum_{\mathcal{K}} \left. \frac{\partial \chi_{\mathcal{J}}}{\partial \mu_{\mathcal{K}}} \frac{\partial \mu_{\mathcal{K}}^\phi}{\partial \phi_{\mathcal{I}}} \right|_{\phi=0}\end{aligned}\quad (7)$$

Explicit computations for $D_{\mathcal{I}, \mathcal{J}}$ are provided in the [Supplementary Information \(SI\)](#). The matrix $D(\chi)$ is symmetric and positive definite, resulting from genotype competition and acting as a diffusion matrix in stochastic processes (see also [SI](#)). Alternatively, $D(\chi)$ can also be seen as a mobility matrix in fluid dynamics, as it links velocity (i.e., cumulant dynamics) to potential force (i.e., the gradient of average fitness)^{10,56}. Eq. (7) suggests that cumulants evolve along the

gradient of average fitness through a matrix that serves as a geometric metric – a picture that was also drawn in the QLE theory¹⁰ – within this generalized setting.

Based on Eq. (7), the extended QLE (exQLE) is derived by truncating the dynamics of cumulants up to order K . In this setting, each row of $D(\chi)$, corresponding to cumulants up to order K , generally involves higher-order cumulants. For instance, the dynamics of first-order cumulants depend on second-, third-, and higher-order terms. However, cumulant dynamics up to order K depend only on a finite set of cumulants, determined by the fitness function. For example, in an additive fitness model ($K^* = 1$), the gradient of the first-order cumulant is constant, and those of higher-order cumulants vanish. Thus, only cumulants up to order $K + K^* = 2$ contribute to $D(\chi)$; higher-order terms (> 2) have no effect on first-order dynamics. Therefore, the equality in Eq. (7) holds as long as $D(\chi)$ includes cumulants up to order $K + K^*$, where K^* is the highest-order cumulant contributing to the fitness function. Similarly, if the goal is to understand the relationship between cumulant dynamics and the gradient of average fitness, and the fitness depends on cumulants up to order K^* , then considering cumulant dynamics up to order $K = K^*$ is necessary (note: the $D(\chi)$ matrix still needs to include cumulants up to order $K + K^* = 2K^*$). As we will discuss in the next section, the exQLE with $K = 2$ under a pairwise fitness function ($K^* = 2$) yields exact results for this reason.

It is important to note that the expression in Eq. (7) is not self-contained, as the dynamics of cumulants up to order K depend on higher-order cumulants up to order $K + K^*$, unless χ includes cumulants of all orders. As a result, it is limited in describing cumulant dynamics over long time periods. To use this equation for simulating cumulant dynamics, the higher-order cumulants (beyond order K) must be specified externally (e.g., assumed to be zero or random) or described by using lower-order cumulants to make the equation self-contained.

Extended QLE: the $K = 2$ case

To illustrate the extension of QLE theory, we consider the $K = 2$ case, where cumulants up to the second order can dynamically evolve, while higher-order cumulants are small and rapidly reach equilibria. We assume a fitness function that depends on cumulants up to order $K^* > 2$ and an arbitrary genotype distribution. Under these conditions, the dynamics of χ_i are given by:

$$\begin{aligned}\dot{\chi}_i &= \partial_{\phi_i} \langle F \rangle_\phi|_{\phi=0} \\ &\simeq \sum_k \chi_{ik} \partial_{\chi_k} \langle F \rangle + \sum_{k < l} \chi_{ikl} \partial_{\chi_{kl}} \langle F \rangle.\end{aligned}\quad (8)$$

Similarly, the dynamics of χ_{ij} follow:

$$\begin{aligned}\dot{\chi}_{ij} &= \partial_{\phi_i} \partial_{\phi_j} \langle F \rangle_\phi|_{\phi=0} \\ &\simeq \sum_k \chi_{ijk} \partial_{\chi_k} \langle F \rangle + \sum_{k < l} (\chi_{ijkl} + \chi_{ikl} \chi_{jl} + \chi_{il} \chi_{jk}) \partial_{\chi_{kl}} \langle F \rangle.\end{aligned}\quad (9)$$

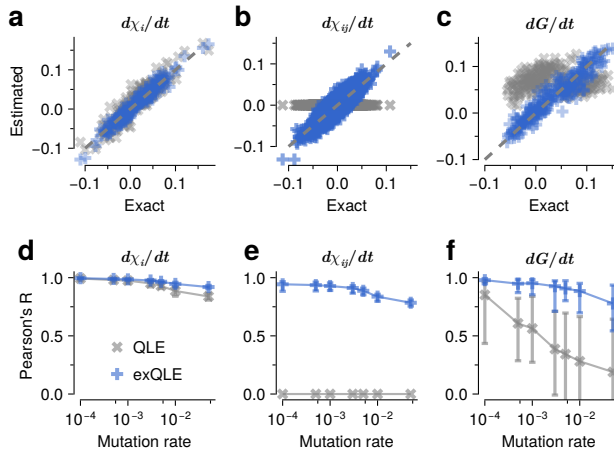


Fig. 1. The accuracy of cumulant and trait dynamics by comparing estimated and exact values. To examine the accuracy of the exQLE framework, we consider a fitness function that depends on interactions up to the fourth-order, providing a non-trivial test case. Genetic sequences were simulated using the Wright–Fisher (WF) process, incorporating mutation, recombination, and selection determined by this fitness function. Simulation conditions are detailed at the [SI](#). This presents the dynamics of first-order cumulants (a), second-order cumulants (b), and a random trait defined below (c), comparing results from exact calculations based on Price’s equation Eq. (2) with those from the exQLE (with $K = 2$) and QLE ($K = 1$). Unlike the QLE case, exQLE closely match the exact dynamics for all cases. For the random trait, which is a pairwise function with parameters drawn from a normal distribution (see [SI](#)), exQLE can accurately capture the dynamics, while QLE cannot. To systematically assess accuracy, we performed 10 independent WF simulations and estimated the R values across multiple mutation rates (Fig. 1d-f). Overall, exQLE consistently outperformed QLE, maintaining higher R values across all mutation rates.

Details of the derivation Eq. (9) are provided in [SI](#). If the average fitness function is characterized by cumulants up to second-order, the relations in Eq. (8) and Eq. (9) hold exactly. Under this extended QLE framework, the dynamics of any arbitrary trait G is given as:

$$\frac{d\langle G \rangle}{dt} \simeq \sum_i \dot{\chi}_i \partial_{\chi_i} \langle G \rangle + \sum_{ij} \dot{\chi}_{ij} \partial_{\chi_{ij}} \langle G \rangle.$$

The dynamics effectively align with gradients of the average fitness surface and average traits. The dynamics of cumulants are characterized by a symmetric matrix $D(\chi)$, such that

$$\dot{\chi} \simeq D(\chi) \nabla_{\chi} \langle F \rangle$$

$$D(\chi) = \begin{pmatrix} \chi_{ik} & \chi_{ikl} \\ \chi_{ijk} & \chi_{ijkl} + \chi_{ik}\chi_{jl} + \chi_{il}\chi_{jk} \end{pmatrix}. \quad (10)$$

Here, the indices i, j, k, l spans all combinations: the top-left block χ_{ik} spans rows and columns 1 to L ; the top-right spans rows 1 to L , columns $L+1$ to $L(L+1)/2$; and the bottom-right spans rows and columns $L+1$ to $L(L+1)/2$. Although the interpretation of the gradient of average fitness and the mobility matrix is absent, equations equivalent to Eq. (8) and Eq. (9) can be found in ref. [57](#).

To examine how the exQLE framework incorporates the second-order cumulant dynamics and enhances the descriptive capacity of population evolution, we numerically compared the cumulant dynamics derived in Eq. (8) and Eq. (9)

with the exact cumulant dynamics obtained from Price’s equation Eq. (2). As we discussed earlier, the expressions Eq. (8) and Eq. (9) are exact when $K = K^* = 2$, and the $D(\chi)$ includes cumulants up to the 4-th order, corresponding to $K + K^*$. Therefore, as a non-trivial example, we considered a fitness function incorporating third- and fourth-order interactions between sites (Fig. 1). The first- and second-order cumulant dynamics derived from exQLE closely correlate with those obtained from the exact calculations, whereas the original QLE framework fails to accurately describe the cumulant dynamics (Fig. 1a-b). As an example of a more general trait, we evaluated the dynamics of a trait defined as a function of first- and second-order cumulants (its mathematical definition is provided in [SI](#)). The results demonstrate that trait dynamics derived from exQLE align well with the exact dynamics, whereas QLE, which excludes second-order cumulant dynamics, does not (Fig. 1c).

To assess the accuracy of exQLE in capturing cumulant and trait dynamics, we analyzed the correlation between the estimated $\dot{\chi}_i, \dot{\chi}_{ij}$ and random traits across multiple mutation rates. Increasing mutation rates lead to a greater number of genotypes, effectively enhancing the presence of finite higher-order cumulants. The Pearson’s R values comparing those from the exact results and estimated ones based on the exQLE framework achieve consistently higher values than those from the QLE method across various mutations (Fig. 1d-f).

Naive computation of dynamics under higher-order fitness is computationally challenging; therefore, we also propose an efficient method in [SI](#).

Infer fitness parameters

We now illustrate how to infer fitness parameters $s = ((s_i), (s_{ij})_{i < j}, \dots)$ from cumulant dynamics. As discussed at the end of the section, the core idea parallels the derivation of the recently proposed marginal path-likelihood (MPL) method [49,50](#). A more mathematically explicit discussion is also provided in [SI](#).

So far, our analysis has assumed deterministic dynamics. However, under finite population size N , stochasticity must be incorporated. To account for this effects, the cumulant dynamics can be represented as a Langevin equation:

$$\dot{\chi} = D(\chi) \nabla_{\chi} \langle F \rangle + \eta(t), \quad (11)$$

where $\eta(t)$ is Gaussian noise, satisfying with $\langle \eta_{\mathcal{J}(t)} \eta_{\mathcal{K}(t')} \rangle = N^{-1} D_{\mathcal{J}, \mathcal{K}}(\chi(t)) \delta(t - t')$. This form of noise arises under the WF process and has been utilized in the prior works [10,49,50](#).

Due to stochasticity, the system traces varied cumulant trajectories over time. Let t_k denote discretize time points, and define $\Delta t_k := t_{k+1} - t_k$. The probability distribution of these trajectories is governed by the Fokker–Planck equation, derived from the Langevin dynamics [58](#). This equation provides the probability density $P(\chi(t_{k+1}), t_{k+1} | \chi(t_k), t_k)$, which is Gaussian, with mean determined by the deterministic dynamics $\chi(t_k) + \Delta t_k \nabla_{\chi} \langle F \rangle(t_k)$ and covariance given

by $N^{-1} D(\chi(t_k))$.

Assuming a Markov process, the likelihood of a full cumulant trajectory is given by the product of these probability densities:

$$P((\chi(t_k))_{k=0}^K) \propto e^{-N\mathcal{S}((\chi(t_k))_{k=0}^K)}, \quad (12)$$

where \mathcal{S} is a time integral of a quadratic function of $\Delta\chi(t_k) := \chi(t_{k+1}) - \chi(t_k)$ and depends quadratically on $\nabla_\chi \langle F \rangle$ and thus on s .

Therefore, the fitness parameters that maximize the likelihood are obtained by solving the following linear equation:

$$\begin{aligned} \hat{s} &= \arg \max_s P((\chi(t_k))_{k=0}^K) \\ &= \left(\sum_{k=0}^K \Delta t_k \tilde{D}(\chi(t_k)) \right)^{-1} \sum_{k=0}^K \Delta\chi(t_k). \end{aligned} \quad (13)$$

where the matrix $\tilde{D}(\chi)$ is defined such that $\tilde{D}(\chi)s = D(\chi)\nabla_\chi \langle F \rangle$.

In the $K = 2$ case, the maximum likelihood equation can be expressed as an explicit form, which we can use to infer s under WF process with mutation and recombination. By reintroducing the expected cumulant changes due to mutation and recombination, as provided in prior works^{10?}, the maximum likelihood equation becomes:

$$\begin{aligned} \sum_{k=0}^K \binom{\Delta\chi_i(t_k)}{\Delta\chi_{ij}(t_k)} + \sum_{k=0}^K \Delta t_k \binom{2\mu\chi_i(t_k)}{(4\mu + rc_{ij})\chi_{ij}(t_k)} \\ = \sum_{k=0}^K \Delta t_k \tilde{D}(\chi(t_k))s \end{aligned} \quad (14)$$

with $\tilde{D}(\chi)$ derived from the matrix $D(\chi)$ in Eq. (10), expressed explicitly as:

$$\tilde{D}(\chi) = \begin{pmatrix} \chi_{ik} & \chi_{ikl} + \chi_{ik}\chi_{il} + \chi_{il}\chi_{ik} \\ \chi_{ijk} & \chi_{ijkl} + \chi_{ik}\chi_{jl} + \chi_{il}\chi_{jk} + \chi_{ijk}\chi_{il} + \chi_{ijl}\chi_{ik} \end{pmatrix}. \quad (15)$$

Notably, the MPL framework yields the same linear equation Eq. (14) and Eq. (15), upon transforming from the 0/1 basis and moment representation to the $-/+$ basis and cumulants^{50,59}. This equivalence holds true as long as both MPL and exQLE derive exact dynamics, which is guaranteed under $K = K^*$, and follow the same logical structure: deriving the Fokker–Planck equation and maximizing the likelihood of cumulant trajectory.

The only slight difference, beyond mathematical conventions, is that exQLE derives the Langevin equation directly from cumulant dynamics for arbitrary order K , whereas MPL formulates the Fokker–Planck equation from the WF process under the diffusion limit. Nevertheless, the Langevin formulation can also be derived within MPL via the same diffusion approximation⁶⁰.

One advantage of using the cumulant-based approach is that the equation of motion can be systematically approximated by reducing the effects of higher-order cumulants in

an order-by-order manner. For example, given the expression Eq. (14), it is relevant to consider the scenario where cumulants beyond the second order are negligible. In this case, the mobility matrix depends only on second-order cumulants, leading to

$$\begin{aligned} \dot{\chi}_i &\simeq \sum_k s_k \chi_{ik} + \sum_{k < l} s_{kl} \chi_{ik} \chi_{il} - 2\mu \chi_i \\ \dot{\chi}_{ij} &\simeq \sum_{k < l} s_{kl} (\chi_{il} \chi_{jk} + \chi_{jl} \chi_{ik}) - (4\mu + rc_{ij}) \chi_{ij}. \end{aligned} \quad (16)$$

When considering only up to second-order cumulants, the dependency of second-order cumulant dynamics on additive selection disappears, as also observed in the previous multi-locus QLE study¹⁰. The absence of additive fitness dependency in second-order cumulant dynamics, which ultimately enables a closed-form expression for epistasis^{10,57}, arises because epistatic effects are coupled with third-order cumulants. By ignoring third-order cumulant dynamics, cumulant evolution becomes effectively independent of additive fitness effects. Suppose we assume steady-state conditions in χ_{ij} and further approximate $\sum_{k < l} s_{kl} \chi_{il} \chi_{jk} \simeq s_{ij} \chi_{ii} \chi_{jj}$. In this case, we recover the identical solution as the QLE epistasis model with Gaussian closure (GC) scheme, which drops more than second-order cumulants^{51,61}, which is given as:

$$s_{ij} = \frac{4\mu + rc_{ij}}{\chi_{ii} \chi_{jj}} \chi_{ij}. \quad (17)$$

To evaluate how accurately the exQLE inference framework, represented by Eq. (14), and the exQLE with GC scheme (exQLEGc), represented by Eq. (16), can infer fitness parameters including selection and epistatic coefficients, we performed 100 independent WF simulations under a pairwise fitness function across multiple mutation rates. This allows us to systematically assess the correlation between inferred coefficients and ground-truth fitness parameters. **Supplementary Fig. S1** also illustrates the results from the $K^* = 4$ case.

Overall, exQLE and exQLEGc achieve similar inference accuracy (accuracy of the forward simulation using exQLEGc can be found in **Supplementary Fig. S2**). For selection coefficients, the average Pearson's R values range from 0.74 to 0.87, with the lowest R value occurring at smaller mutation rates and the highest R values at the highest mutation rate ($\mu = 0.05$) (**Fig. 2a**). For epistatic inference, mutation rates noticeably influence R values, with the lowest R value of 0.15 occurring at the lowest mutation rate. Higher mutation rates yielded higher R values, up to a maximum of 0.79 (**Fig. 2b**). Genetic diversity is measured by the average entropy across all sites, assuming that the sites are independent of one another, and varies with mutation rates in a similar manner to the Pearson's R values for inferred epistasis. This suggests that increased mutation rates diversify the population, effectively increasing the number of distinct genotypes, enhancing the precision of cumulant estimation, and resulting in higher R values for the epistasis inference (**Fig. 2d**). The inferred fitness values, obtained from

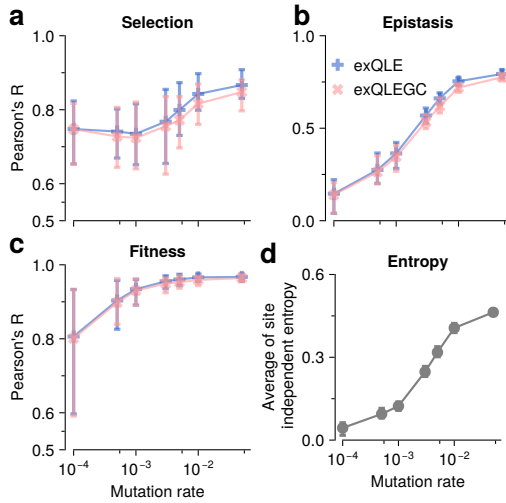


Fig. 2. Pearson's R values comparing inferred and ground-truth fitness values for selection coefficients (a) and epistatic coefficients (b), as well as overall fitness values (c). Here, we consider the case $K^* = 2$, while the case $K^* = 4$ is provided in **Supplementary Fig. S2**. We fixed the recombination rate at $r = 3 \times 10^{-3}$ per generation per site, as recombination does not significantly influence inference accuracy, particularly for exQLE. Inferred selection and epistatic coefficients were obtained from temporal genetic sequences generated using the WF process, incorporating recombination, mutations, and selection, based on the expression of the cumulant dynamics Eq. (14) (for QLEG C, Eq. (16) is used). The R values, used as a measure of inference accuracy for selection coefficients, remain consistently high across all tested mutation rates. However, the R values for inferred epistatic coefficients show significant dependence on mutation rates. This mutation rate dependency likely arises from increased genetic diversity, which improves the estimation of higher order cumulants. The entropy profile defined as the entropy of independent site frequency $\nu_i = (1 + \chi_i)/2$ is given by $S = -\frac{1}{L} \sum_{i=1}^L \langle \nu_i(t) \log(\nu_i(t)) \rangle_t$, where $\langle \cdot \rangle_t$ represents the average over time points (every 50 generations between generations 1,500 and 2,000). This entropy profile serves as a metric of genetic diversity and closely resembles the profile of R values for inferred epistatic coefficients. This correlation suggests that an increase in mutation rate increases genetic diversity, thereby enhancing the inference accuracy for epistasis.

inferred selection and epistatic coefficients as well as genetic sequences, also increase with mutation rates, though they exceed 0.81 with a maximum value of 0.97 at the highest mutation rate.

Discussion

Quantitatively understanding how fundamental evolutionary forces, such as selection, mutation, and recombination, shape the evolution of populations and phenotypic traits, is a central question in evolutionary biology^{3,62–64}. While considering multilocus effects is crucial for capturing the complexity of genetic evolution, and growing evidence shows that most phenotypic traits are governed by many alleles across different loci^{34–48}, many foundational results were based on single-locus or two-locus models^{1,7,60,65–67}.

Existing studies of genetic evolution in multilocus populations often assume that the non-random association between alleles in different loci, known as linkage disequilibrium (LD), rapidly vanishes and is negligibly small^{6,15,65,68}. Although these studies provide valuable insights into genetic evolution, they do not apply to collective evolution across different sites, which involves complex and rich phenomena^{20–23,69,70}.

Quasi-linkage equilibrium (QLE), where the LD is present but is weak and rapidly converges to the equilibrium state^{4,7,8,10,12–16}, allows for exploring collective allele evolution while simplifying mathematical structures.

However, the existing QLE theories have limitations. Populations can reach the QLE phase only when the recombination rate is much larger than the selection¹², and epistasis is also smaller than the recombination rate⁹, which significantly restricts the application of the QLE phase. In the inter-host evolution of SARS-CoV-2, selective pressures are likely strong, but the recombination rate is effectively zero, leading to significant LD⁷¹. Although the human immunodeficiency virus exhibits a higher recombination rate^{72,73}, selective pressure can be significant, and often substantial LD persists over many years^{49,72,74,75}. Additionally, the recent progress in high-throughput deep mutational scanning to measure functional effects revealed the prevalence of widespread epistatic epistasis in viral and bacterial population in wild, and bacterial populations^{27,44,76,77}. Collectively, this evidence suggests that the QLE assumption violates conditions where LDs or higher-order cumulants of alleles across loci are unlikely to converge to equilibrium rapidly, and the timescales of higher-order cumulants and individual allele frequencies are not well separated.

Here, we present an extension of QLE theory, exQLE, which generalizes QLE to allow cumulants up to any order K to evolve dynamically. To demonstrate this, we first expressed the cumulant dynamics for arbitrary orders and arbitrary genotype distributions (corresponding to Eq. (7)), providing a geometric interpretation of the dynamics and insights into when the expression can be exact. The resulting matrix $D(\chi)$ servers as a geometric metric, and its general form is detailed in the **Supplementary Information**. The exQLE formulation naturally arises from Eq. (7) under conditions or genotype distributions where cumulants of order greater than K evolve rapidly toward equilibria, while the K -th order and lower cumulants remain dynamically changing. As an example of exQLE, we investigated the case $K = 2$, focusing on fitness functions whose averages depend on cumulants up to order $K^* = 4$ (noting that the $K^* = 2$ case is trivially exact). Under this condition, the $K = 2$ exQLE framework can accurately demonstrate the cumulant dynamics, a capability that the standard QLE framework lacks.

The derived cumulant dynamics enable inference of fitness parameters by maximizing the likelihood of observed cumulant trajectories over evolutionary time, closely resembling the marginal path-likelihood (MPL) method recently proposed in^{49,50,59}. Despite differences in mathematical conventions between MPL and the exQLE-based approach, both yield effectively identical inference results.

Since the equations for cumulant dynamics are expressed as combinations of cumulants, their complexity can be systematically reduced by suppressing cumulants in a stratified, order-by-order manner. To achieve this, we employed an alternative Gaussian closure scheme, in which cumulants beyond the second order are assumed to be absent. The resulting novel family of inference methods accurately estimates

selection and epistatic coefficients.

We could not fully explore the equilibrium distribution in the exQLE framework, in this work. Similar to the prior work¹⁰, an explicit expression for the equilibrium distribution $Q(\chi)$ could be derived from the forward Kolmogorov equation, which is characterized by K -th order cumulant dynamics, such that $\partial_t Q(\chi, t) = \nabla_{\chi}^{\top} j(\chi, t)$, where $j(\chi, t)$ is the probability current. The equilibrium distribution can be obtained from the condition $j(\chi) = 0$. For example, when $K = 2$, the equilibrium distribution includes the interactions between first-order cumulants in an exponential function. Similar to the equilibrium distribution under QLE¹⁰, the equilibrium distribution under exQLE also features an exponential form and an entropic term. Although, the general form of the equilibrium distribution remains conjectural, it likely depends on higher-order epistatic interactions between all possible combinations of cumulants up to order K , shaped by cumulants, mutation rates, and recombination rates, and appearing within the exponential function.

ACKNOWLEDGEMENTS

The work of K.S.S. and J.P.B. reported in this publication was supported by the National Institute of General Medical Sciences of the National Institutes of Health under Award Number R35GM138233. M.P. was funded by the European Union (ERC, CHORAL, project number 101039794). Views and opinions expressed are however those of the authors only and do not necessarily reflect those of the European Union or the European Research Council. Neither the European Union nor the granting authority can be held responsible for them.

References

- Wright, S. Evolution in mendelian populations. *Genetics* **16**, 97 (1931).
- Fisher, R. A. *The genetical theory of natural selection: a complete variorum edition* (Oxford University Press, 1999).
- Walsh, B. & Lynch, M. *Evolution and selection of quantitative traits* (Oxford University Press, 2018).
- Crow, J. F. *An introduction to population genetics theory* (Scientific Publishers, 2017).
- Lewontin, R. C. & Kojima, K.-i. The evolutionary dynamics of complex polymorphisms. *Evolution* **45**, 458–472 (1990).
- Barton, N. H. & Turelli, M. Evolutionary quantitative genetics: how little do we know. *Annual review of genetics* **23**, 337–370 (1992).
- Kimura, M. Attainment of quasi linkage equilibrium when gene frequencies are changing by natural selection. *Genetics* **52**, 875 (1965).
- Barton, N. H. A general model for the evolution of recombination. *Genetics Research* **65**, 123–144 (1995).
- Neher, R. A. & Shraiman, B. I. Competition between recombination and epistasis can cause a transition from allele to genotype selection. *Proceedings of the National Academy of Sciences* **106**, 6866–6871 (2009).
- Neher, R. A. & Shraiman, B. I. Statistical genetics and evolution of quantitative traits. *Reviews of Modern Physics* **83**, 1283 (2011).
- Nagylaki, T. Quasilinear equilibrium and the evolution of two-locus systems. *Proceedings of the National Academy of Sciences* **71**, 526–530 (1974).
- Barton, N. H. & Otto, S. P. Evolution of recombination due to random drift. *Genetics* **169**, 2353–2370 (2005).
- Barton, N. H. & Turelli, M. Natural and sexual selection on many loci. *Genetics* **127**, 229–255 (1991).
- Turelli, M. & Barton, N. H. Genetic and statistical analyses of strong selection on polygenic traits: what, me normal? *Genetics* **138**, 913–941 (1994).
- Kirkpatrick, M., Johnson, T. & Barton, N. General models of multilocus evolution. *Genetics* **161**, 1727–1750 (2002).
- Nagylaki, T. The evolution of multilocus systems under weak selection. *Genetics* **134**, 627–647 (1993).
- Nagylaki, T., Hofbauer, J. & Brunovský, P. Convergence of multilocus systems under weak epistasis or weak selection. *Journal of mathematical biology* **38**, 103–133 (1999).
- Zeng, H.-L. & Aurell, E. Inferring genetic fitness from genomic data. *Physical Review E* **101**, 052409 (2020).
- Zeng, H.-L., Dichi, V., Rodríguez Horta, E., Thorell, K. & Aurell, E. Global analysis of more than 50,000 sars-cov-2 genomes reveals epistasis between eight viral genes. *Proceedings of the National Academy of Sciences* **117**, 31519–31526 (2020).
- Smith, J. M. & Haigh, J. The hitch-hiking effect of a favourable gene. *Genetics Research* **23**, 23–35 (1974).
- Barton, N. H. Genetic hitchhiking. *Philosophical Transactions of the Royal Society of London. Series B: Biological Sciences* **355**, 1553–1562 (2000).
- Hill, W. G. & Robertson, A. The effect of linkage on limits to artificial selection. *Genetics Research* **8**, 269–294 (1966).
- Felsenstein, J. The evolutionary advantage of recombination. *Genetics* **78**, 737–756 (1974).
- Husain, K. & Murugan, A. Physical constraints on epistasis. *Molecular Biology and Evolution* **37**, 2865–2874 (2020).
- Kryazhimskiy, S. Emergence and propagation of epistasis in metabolic networks. *Elife* **10**, e60200 (2021).
- Poelwijk, F. J., Krishna, V. & Ranganathan, R. The context-dependence of mutations: a linkage of formalisms. *PLoS computational biology* **12**, e1004771 (2016).
- Otwinskiowski, J., McCandlish, D. M. & Plotkin, J. B. Inferring the shape of global epistasis. *Proceedings of the National Academy of Sciences* **115**, E7550–E7558 (2018).
- Zhou, J. *et al.* Higher-order epistasis and phenotypic prediction. *Proceedings of the National Academy of Sciences* **119**, e2204233119 (2022).
- Rijal, K. *et al.* Inferring genotype-phenotype maps using attention models. *arXiv preprint arXiv:2504.10388* (2025).
- Lyons, D. M., Zou, Z., Xu, H. & Zhang, J. Idiosyncratic epistasis creates universals in mutational effects and evolutionary trajectories. *Nature Ecology & Evolution* **4**, 1685–1693 (2020).
- Reddy, G. & Desai, M. M. Global epistasis emerges from a generic model of a complex trait. *Elife* **10**, e64740 (2021).
- Johnson, M. S., Reddy, G. & Desai, M. M. Epistasis and evolution: recent advances and an outlook for prediction. *BMC biology* **21**, 120 (2023).
- Diaz-Colunga, J. *et al.* Global epistasis on fitness landscapes. *Philosophical Transactions of the Royal Society B* **378**, 20220053 (2023).
- Chou, H.-H., Chiu, H.-C., Delaney, N. F., Segre, D. & Marx, C. J. Diminishing returns epistasis among beneficial mutations decelerates adaptation. *Science* **332**, 1190–1192 (2011).
- Khan, A. I., Dinh, D. M., Schneider, D., Lenski, R. E. & Cooper, T. F. Negative epistasis between beneficial mutations in an evolving bacterial population. *Science* **332**, 1193–1196 (2011).
- Kryazhimskiy, S., Rice, D. P., Jerison, E. R. & Desai, M. M. Global epistasis makes adaptation predictable despite sequence-level stochasticity. *Science* **344**, 1519–1522 (2014).
- Olson, C. A., Wu, N. C. & Sun, R. A comprehensive biophysical description of pairwise epistasis throughout an entire protein domain. *Current biology* **24**, 2643–2651 (2014).
- Starr, T. N., Flynn, J. M., Mishra, P., Bolon, D. N. & Thornton, J. W. Pervasive contingency and entrenchment in a billion years of hsp90 evolution. *Proceedings of the National Academy of Sciences* **115**, 4453–4458 (2018).
- Park, Y., Metzger, B. P. & Thornton, J. W. Epistatic drift causes gradual decay of predictability in protein evolution. *Science* **376**, 823–830 (2022).
- Bakerlee, C. W., Nguyen Ba, A. N., Shulgina, Y., Rojas Echenique, J. I. & Desai, M. M. Idiosyncratic epistasis leads to global fitness-correlated trends. *Science* **376**, 630–635 (2022).
- Sailer, Z. R. & Harms, M. J. High-order epistasis shapes evolutionary trajectories. *PLoS computational biology* **13**, e1005541 (2017).
- Poelwijk, F. J., Socolich, M. & Ranganathan, R. Learning the pattern of epistasis linking genotype and phenotype in a protein. *Nature communications* **10**, 4213 (2019).
- Phillips, A. M. *et al.* Binding affinity landscapes constrain the evolution of broadly neutralizing anti-influenza antibodies. *Elife* **10**, e71393 (2021).
- Moulana, A. *et al.* The landscape of antibody binding affinity in sars-cov-2 omicron ba. 1 evolution. *Elife* **12**, e83442 (2023).
- Phillips, A. M. *et al.* Hierarchical sequence-affinity landscapes shape the evolution of breadth in an anti-influenza receptor binding site antibody. *Elife* **12**, e83628 (2023).
- Yang, G. *et al.* Higher-order epistasis shapes the fitness landscape of a xenobiotic-degrading enzyme. *Nature Chemical Biology* **15**, 1120–1128 (2019).
- Buda, K., Miton, C. M. & Tokuriki, N. Pervasive epistasis exposes intramolecular networks in adaptive enzyme evolution. *Nature Communications* **14**, 8508 (2023).
- Schulz, S., Tan, T. J., Wu, N. C. & Wang, S. Epistatic hotspots organize antibody fitness landscape and boost evolvability. *Proceedings of the National Academy of Sciences* **122**, e2413884122 (2025).
- Sohail, M. S., Louie, R. H., McKay, M. R. & Barton, J. P. Mpi resolves genetic linkages in fitness inference from complex evolutionary histories. *Nature biotechnology* **39**, 472–479 (2021).
- Sohail, M. S., Louie, R. H., Hong, Z., Barton, J. P. & McKay, M. R. Inferring epistasis from genetic time-series data. *Molecular biology and evolution* **39**, msac199 (2022).
- Mauri, E., Cocco, S. & Monasson, R. Gaussian closure scheme in the quasi-linkage equilibrium regime of evolving genome populations. *Europhysics Letters* **132**, 56001 (2021).
- Murray, J. D. *Mathematical biology: I. An introduction*, vol. 17 (Springer Science & Business Media, 2007).
- Ewens, W. J. *Mathematical population genetics: theoretical introduction*, vol. 1 (Springer, 2004).
- Price, G. R. Fisher's 'fundamental theorem' made clear. *Annals of human genetics* **36**, 129–140 (1972).
- Robertson, A. A mathematical model of the culling process in dairy cattle.

- Animal Science* **8**, 95–108 (1966).
- 56. Durlofsky, L., Brady, J. F. & Bossis, G. Dynamic simulation of hydrodynamically interacting particles. *Journal of fluid mechanics* **180**, 21–49 (1987).
 - 57. Dichiø, V., Zeng, H.-L. & Aurell, E. Statistical genetics in and out of quasi-linkage equilibrium. *Reports on Progress in Physics* **86**, 052601 (2023).
 - 58. Risken, H. Fokker-planck equation. In *The Fokker-Planck equation: methods of solution and applications*, 63–95 (Springer, 1989).
 - 59. Shimagaki, K. S. & Barton, J. P. Efficient epistasis inference via higher-order covariance matrix factorization. *Genetics* **iyaf118** (2025).
 - 60. Kimura, M. Diffusion models in population genetics. *Journal of Applied Probability* **1**, 177–232 (1964).
 - 61. Zeng, H.-L. *et al.* Inferring epistasis from genomic data with comparable mutation and outcrossing rate. *Journal of Statistical Mechanics: Theory and Experiment* **2021**, 083501 (2021).
 - 62. Lande, R. & Arnold, S. J. The measurement of selection on correlated characters. *Evolution* 1210–1226 (1983).
 - 63. Nourmohammad, A., Held, T. & Lässig, M. Universality and predictability in molecular quantitative genetics. *Current opinion in genetics & development* **23**, 684–693 (2013).
 - 64. Nourmohammad, A. *et al.* Adaptive evolution of gene expression in drosophila. *Cell reports* **20**, 1385–1395 (2017).
 - 65. Wright, S. The distribution of gene frequencies in populations. *Proceedings of the National Academy of Sciences* **23**, 307–320 (1937).
 - 66. Crow, J. F. & Kimura, M. Evolution in sexual and asexual populations. *The American Naturalist* **99**, 439–450 (1965).
 - 67. Ohta, T. & Kimura, M. Linkage disequilibrium at steady state determined by random genetic drift and recurrent mutation. *Genetics* **63**, 229 (1969).
 - 68. Lynch, M., Walsh, B. *et al.* *Genetics and analysis of quantitative traits*, vol. 1 (Sinauer Sunderland, MA, 1998).
 - 69. Good, B. H., Walczak, A. M., Neher, R. A. & Desai, M. M. Genetic diversity in the interference selection limit. *PLoS genetics* **10**, e1004222 (2014).
 - 70. Good, B. H. Linkage disequilibrium between rare mutations. *Genetics* **220**, iyac004 (2022).
 - 71. Lee, B. *et al.* Inferring effects of mutations on sars-cov-2 transmission from genomic surveillance data. *Nature Communications* **16**, 441 (2025).
 - 72. Zanini, F. *et al.* Population genomics of intrapatient hiv-1 evolution. *eLife* **4**, e11282 (2015).
 - 73. Romero, E. V. & Feder, A. F. Elevated hiv viral load is associated with higher recombination rate in vivo. *Molecular Biology and Evolution* **41**, msad260 (2024).
 - 74. Shimagaki, K. S., Lynch, R. M. & Barton, J. P. Parallel hiv-1 fitness landscapes shape viral dynamics in humans and macaques that develop broadly neutralizing antibodies. *eLife* **14** (2025).
 - 75. Shimagaki, K. & Barton, J. P. Bézier interpolation improves the inference of dynamical models from data. *Physical Review E* **107**, 024116 (2023).
 - 76. Starr, T. N. *et al.* Deep mutational scanning of sars-cov-2 receptor binding domain reveals constraints on folding and ace2 binding. *cell* **182**, 1295–1310 (2020).
 - 77. Moullana, A. *et al.* Compensatory epistasis maintains ace2 affinity in sars-cov-2 omicron ba. 1. *Nature communications* **13**, 7011 (2022).

Supplementary Information

Stochastic Processes in Population genetics

Following the convention of previous studies^{78,79}, we represent genetic sequences as $\mathbf{g} \in \{-1, +1\}^L$, where L is the sequence length. This $-/+$ encoding is commonly used in the physics literature. For a genotype $a \in \{1, \dots, M\}$ with $M = 2^L$, and corresponding sequence \mathbf{g}^a , the fitness is defined as $F^a = F(\mathbf{g}^a)$. We consider the following general form for the fitness function:

$$F(\mathbf{g}) = \bar{F} + \sum_i s_i g_i + \sum_{i < j} s_{ij} g_i g_j + \dots , \quad (\text{S1})$$

where the fitness parameters s_i and s_{ij} represent selection coefficients and pairwise epistatic interactions, respectively. Interactions beyond pairwise, such as s_{ijk}, s_{ijkl}, \dots , can also occur, and we refer to these as higher-order epistatic interactions. For simplicity, we denote fitness parameters generically as s_e , where the index e may represent a single-site effect (i), pairwise (i, j), three-way (i, j, k), four-way (i, j, k, l), and so on.

To model the evolution of genetic sequences, we employed the Wright–Fisher (WF) process, a foundational stochastic model in population genetics that captures reproduction dynamics⁸⁰. The WF process describes the evolution of a population with fixed size N . At time t_k (the parent generation), the population is represented by genotype counts $(n_1(t_k), \dots, n_M(t_k))^\top = (n_a(t_k))_a^M$, which give rise to the next generation at time t_{k+1} , denoted $(n_a(t_{k+1}))_a^M$.

Demographic noise, or genetic drift, arises from stochastic sampling and is on the order of $\mathcal{O}(1/N)$. It can be quantified through fluctuations in genotype frequencies, defined as $\nu_a = n_a/N$. Mathematically, the WF process is a discrete-time multinomial process. Additional evolutionary forces, including selection (with fitness $F(\mathbf{g})$), mutation, and recombination, can be incorporated. Mutation and recombination occur at rates μ and r per site per generation, respectively.

Let $\boldsymbol{\nu} = \mathbf{n}/N$ denote the genotype frequency vector, $p_a(\boldsymbol{\nu} | F, \mu, r)$ denote the probability that genotype a is selected, given the current genotype frequencies $\boldsymbol{\nu}$, fitness function $F(\mathbf{g})$, and evolutionary forces such as mutation and recombination (defined below). Then, the WF process can be expressed as:

$$p((\boldsymbol{\nu}(t_k))_{k=0}^K | F, \mu, r, N) = \prod_{k=0}^{K-1} p(\boldsymbol{\nu}(t_{k+1}) | \boldsymbol{\nu}(t_k); F, \mu, r, N) , \quad (\text{S2})$$

whre

$$p(\boldsymbol{\nu}(t_{k+1}) | \boldsymbol{\nu}(t_k); F, \mu, r, N) = N! \prod_a \frac{p_a(\boldsymbol{\nu}(t_k) | F, \mu, r)^{N\nu_a(t_{k+1})}}{[N\nu_a(t_{k+1})]!} . \quad (\text{S3})$$

Let $y_a(\boldsymbol{\nu}; r)$ denote the probability that recombination events produce genotype a , which can be expressed as:

$$y_a(\boldsymbol{\nu}; r) = (1 - r)^{L-1} \nu_a + \left(1 - (1 - r)^{L-1}\right) \sum_{b,c} R_{a|b,c} \nu_b \nu_c . \quad (\text{S4})$$

The selection probability is then given by:

$$p_a(\boldsymbol{\nu} | F, \mu, r) = \frac{y_a(\boldsymbol{\nu}; r) F_a + \mu \sum_{b: d_{ab}=1} [y_b(\boldsymbol{\nu}; r) F_b - y_a(\boldsymbol{\nu}; r) F_a]}{\sum_b y_b(\boldsymbol{\nu}; r) F_b} . \quad (\text{S5})$$

In this expression, d_{ab} denotes the Hamming distance between genotypes a and b . When the mutation rate μ is low, at most one mutation is expected per individual per generation. As a result, the contribution to the mutation flux in the numerator of Eq. (S5) comes only from genotype pairs that differ by a single mutation (i.e., $d_{ab} = 1$).

Details of simulation conditions

To examine a non-trivial scenario, we considered a higher-order fitness function defined as

$$F(\mathbf{g}) = \bar{F} + \sum_i s_i g_i + \sum_{i < j} s_{ij} g_i g_j + \sum_{i < j < k} s_{ijk} g_i g_j g_k + \sum_{i < j < k < l} s_{ijkl} g_i g_j g_k g_l . \quad (\text{S6})$$

where the fitness coefficients $s_e \in \{-0.03, 0, 0.03\}$ for indices $e = i, (i, j), (i, j, k), (i, j, k, l)$. The number of nonzero coefficients s_e was kept at $\mathcal{O}(L)$ across orders one through four, with L denoting the sequence length. In Fig. 1, to assess the influence of higher-order cumulants on trait dynamics, we also considered random traits defined as

$$G^{\text{Rand}}(\mathbf{g}) = \sum_i a_i g_i + \sum_{i < j} a_{ij} g_i g_j , \quad (\text{S7})$$

where $a_i \sim \mathcal{N}(0, 1/L)$ and $a_{ij} \sim \mathcal{N}(0, 2/L(L-1))$ for all i, j . These coefficients were independently sampled.

The simulation conditions of **Fig. 1** are as follows. Fitness parameters were drawn from the set $\{-0.03, 0, 0.03\}$, while maintaining the number of nonzero parameters at $O(L)$ for each order, where $L = 100$ is the sequence length. The recombination rate was fixed at $r = 3 \times 10^{-3}$ per site per generation, as the results were robust across different recombination rates. In contrast, the simulation outcomes depend on the mutation rate, which we varied between 10^{-4} and 0.05 per site per generation. The population size was set to $N = 10^3$. As we observed no significant variation in cumulant dynamics after 10^3 generations, we sampled genetic sequences every 200 generations between 10^3 and 2×10^3 generations.

Computation of $D_{K,J}(\chi)$ matrix

We now provide a more explicit expression for $D_{\mathcal{I},\mathcal{J}}$. As we noted in the main text, $\mathcal{I}, \mathcal{J}, \mathcal{K}$ are multi-indices over loci, and cumulants and moments of arbitrary order are defined as $\chi_{\mathcal{I}}^\phi = \partial_{\phi_{\mathcal{I}}} \Phi$ and $\mu_{\mathcal{I}}^\phi = e^{-\Phi} \partial_{\phi_{\mathcal{I}}} e^\Phi$, respectively. The general form of cumulant dynamics is given as

$$\begin{aligned} \partial_{\phi_{\mathcal{I}}} \langle F \rangle_{\phi=0} &= \sum_{\mathcal{J}} D_{\mathcal{I},\mathcal{J}} \frac{\partial \langle F \rangle}{\partial \chi_{\mathcal{J}}} \\ D_{\mathcal{I},\mathcal{J}} &= \sum_{\mathcal{K}} \frac{\partial \chi_{\mathcal{J}}}{\partial \mu_{\mathcal{K}}} \left. \frac{\partial \mu_{\mathcal{K}}^\phi}{\partial \phi_{\mathcal{I}}} \right|_{\phi=0} . \end{aligned} \quad (\text{S8})$$

We express moments $\mu_{\mathcal{K}}$ in terms of cumulants since derivatives of cumulants with respect to ϕ are more tractable. Specifically, moments can be written as:

$$\mu_{\mathcal{K}} = \sum_{\pi \in \mathcal{P}(\mathcal{K})} \prod_{B \in \pi} \chi_B . \quad (\text{S9})$$

where $\mathcal{P}(\mathcal{K})$ denotes all partitions of the index set \mathcal{K} . For example, if $\mathcal{K} = \{k_1\}$, then $\mathcal{P}(\mathcal{K}) = \{\{k_1\}\}$. For $\mathcal{K} = \{k_1, k_2\}$, $\mathcal{P}(\mathcal{K}) = \{\{k_1, k_2\}, \{\{k_1\}, \{k_2\}\}\}$, and so on.

Therefore,

$$\left. \frac{\partial \mu_{\mathcal{K}}^\phi}{\partial \phi_{\mathcal{I}}} \right|_{\phi=0} = \sum_{\pi \in \mathcal{P}(\mathcal{K})} \left[\partial_{\phi_{\mathcal{I}}} \prod_{B \in \pi} \chi_B^\phi \right]_{\phi=0} . \quad (\text{S10})$$

To relate cumulants to moments, we use the Faà di Bruno formula:

$$\chi_{\mathcal{J}} = \sum_{\pi \in \mathcal{P}(\mathcal{J})} (-1)^{|\pi|-1} (|\pi|-1)! \prod_{B \in \pi} \mu_B , \quad (\text{S11})$$

from which, we obtain the derivative of cumulants with respect to moments:

$$\frac{\partial \chi_{\mathcal{J}}}{\partial \mu_{\mathcal{K}}} = \sum_{\pi \in \mathcal{P}(\mathcal{J})} (-1)^{|\pi|-1} (|\pi|-1)! \frac{\partial}{\partial \mu_{\mathcal{K}}} \prod_{B \in \pi} \mu_B . \quad (\text{S12})$$

Thus, combining Eq. (S12) and Eq. (S10), we obtain the explicit expression of $D_{\mathcal{I},\mathcal{J}}$ in Eq. (S8). Below, we demonstrate this for specific cases under a pairwise fitness function.

$K = 1$ case

Let us consider a simple $\mathcal{I} = \{i\}, \mathcal{J} = \{j\}$ case. The only partition for $\mathcal{K} = \{j\}$ is $\mathcal{P}(\mathcal{K}) = \{\{j\}\}$, and we obtain:

$$\frac{\partial \chi_j}{\partial \mu_{\mathcal{K}}} = \delta_{\{j\}, \mathcal{K}} ,$$

where $\delta_{\mathcal{K}, \mathcal{L}}$ returns 1 if $\mathcal{K} = \mathcal{L}$, otherwise returns 0. Thus, the D matrix reduces to:

$$D_{i,j} = \sum_{\mathcal{K}} \delta_{\{j\}, \mathcal{K}} \sum_{\pi \in \mathcal{P}(\mathcal{K})} \left[\partial_{\phi_i} \prod_{B \in \pi} \chi_B^\phi \right]_{\phi=0} = \sum_{\mathcal{K}} \delta_{\{j\}, \mathcal{K}} \partial_{\phi_i} \chi_j^\phi |_{\phi=0} = \chi_{ij} .$$

where only $\mathcal{K} = \{j\}$ contributes. Therefore, this result is consistent with the $K = 1$ case.

$K = 2$ case

Since the expression for D_{ij} matches the $K = 1$ case, we consider three additional cases: $\mathcal{I} = \{i, j\}, \mathcal{J} = \{k\}; \mathcal{I} = \{i\}, \mathcal{J} = \{k, l\};$ and $\mathcal{I} = \{i, j\}, \mathcal{J} = \{k, l\}.$

For $\mathcal{I} = \{i, j\}, \mathcal{J} = \{k\}$, we have seen that $\frac{\partial \chi_k}{\partial \mu_{\mathcal{K}}} = \delta_{j,k}$. from the example in $K = 1$ case. Therefore, we have

$$D_{ij,k} = \sum_{\mathcal{K}} \delta_{\{k\}, \mathcal{K}} \left[\partial_{\phi_i} \partial_{\phi_j} \chi_k^\phi \right]_{\phi=0} = \chi_{ijk} .$$

For $\mathcal{I} = \{i\}, \mathcal{J} = \{k, l\}$, the cumulant-moment relation yields,

$$\frac{\partial \chi_{kl}}{\partial \mu_{\mathcal{K}}} = -\chi_l \delta_{\{k\}, \mathcal{K}} - \chi_k \delta_{\{l\}, \mathcal{K}} + \delta_{\{k, l\}, \mathcal{K}} .$$

Therefore,

$$\begin{aligned} D_{i,kl} &= \sum_{\mathcal{K}} (-\chi_l \delta_{\{k\}, \mathcal{K}} - \chi_k \delta_{\{l\}, \mathcal{K}} + \delta_{\{k, l\}, \mathcal{K}}) \left[\partial_{\phi_i} \sum_{\pi \in \mathcal{P}(\mathcal{K})} \prod_{B \in \pi} \chi_B^\phi \right]_{\phi=0} \\ &= -\chi_l \chi_{ik} - \chi_k \chi_{il} + \left[\partial_{\phi_i} (\chi_{kl}^\phi + \chi_k^\phi \chi_l^\phi) \right]_{\phi=0} \\ &= -\chi_l \chi_{ik} - \chi_k \chi_{il} + \chi_{ikl} + \chi_l \chi_{ik} + \chi_k \chi_{il} = \chi_{ikl} . \end{aligned}$$

For $\mathcal{I} = \{i, j\}, \mathcal{J} = \{k, l\}$ case,

$$\begin{aligned} D_{ij,kl} &= \sum_{\mathcal{K}} (-\chi_l \delta_{\{k\}, \mathcal{K}} - \chi_k \delta_{\{l\}, \mathcal{K}} + \delta_{\{k, l\}, \mathcal{K}}) \left[\partial_{\phi_i} \partial_{\phi_j} \sum_{\pi \in \mathcal{P}(\mathcal{K})} \prod_{B \in \pi} \chi_B^\phi \right]_{\phi=0} \\ &= -\chi_l \chi_{ijk} - \chi_k \chi_{ijl} + \left[\partial_{\phi_i} \partial_{\phi_j} (\chi_{kl}^\phi + \chi_k^\phi \chi_l^\phi) \right]_{\phi=0} \\ &= -\chi_l \chi_{ijk} - \chi_k \chi_{ijl} + \chi_{ijkl} + \chi_{ik} \chi_{jl} + \chi_{il} \chi_{jk} + \chi_l \chi_{ijk} + \chi_k \chi_{ijl} \\ &= \chi_{ijkl} + \chi_{ik} \chi_{jl} + \chi_{il} \chi_{jk} . \end{aligned}$$

In summary, we recover the full $D(\chi)$ matrix,

$$D(\chi) = \begin{pmatrix} D_{i,k} & D_{i,kl} \\ D_{ij,k} & D_{ij,kl} \end{pmatrix} = \begin{pmatrix} \chi_{ik} & \chi_{ikl} \\ \chi_{ijk} & \chi_{ijkl} + \chi_{ik} \chi_{jl} + \chi_{il} \chi_{jk} \end{pmatrix} ,$$

consistent with the expression in Eq. (10).

Derivation of Explicit Expressions for First- and Second-Order cumulants under Pairwise Fitness Function

Exact calculation

Here, we derive explicit expressions for the first- and second-order cumulants' equations of motion under the pairwise fitness function and demonstrate that the results derived from the exQLE yield the exact results. Pairwise fitness is defined as:

$$\begin{aligned} F(g) &= \bar{F} + \sum_k s_k g_k + \sum_{k < l} s_{kl} g_k g_l \\ &= \bar{F} + \sum_k s_k g_k + \sum_{k < l} s_{kl} (g_k - \chi_k)(g_l - \chi_l) + \sum_{k < l} s_{kl} (g_k - \chi_k) \chi_l + \sum_{k < l} s_{kl} \chi_k (g_l - \chi_l) + \sum_{k < l} s_{kl} \chi_k \chi_l . \end{aligned} \tag{S13}$$

Derivatives yield:

$$\begin{aligned} \partial_{\chi_i} \langle F \rangle &= s_i + \sum_{l; l > i} s_{il} \chi_l + \sum_{k; k < i} s_{ki} \chi_k, \\ \partial_{\chi_{ij}} \langle F \rangle &= s_{ij} . \end{aligned} \tag{S14}$$

Subtracting,

$$F(g) - \langle F \rangle = \sum_k s_k (g_k - \chi_k) + \sum_{k < l} s_{kl} [(g_k - \chi_k)(g_l - \chi_l) + (g_k - \chi_k)\chi_l + \chi_k(g_l - \chi_l) - \chi_{kl}] \quad (\text{S15})$$

Taking expectations:

$$\begin{aligned} \langle F(g) - \langle F \rangle \rangle &= 0 & , \\ \langle (g_i - \chi_i)(F(g) - \langle F \rangle) \rangle &= \sum_k s_k \chi_{ik} + \sum_{k < l} s_{kl} (\chi_{ikl} + \chi_{ik}\chi_l + \chi_k\chi_{il}) & , \\ \langle (g_i - \chi_i)(g_j - \chi_j)(F(g) - \langle F \rangle) \rangle &= \sum_k s_k \chi_{ijk} + \sum_{k < l} s_{kl} (m_{ijkl} + \chi_{ijk}\chi_l + \chi_k\chi_{ijl} - \chi_{ij}\chi_{kl}) & . \end{aligned} \quad (\text{S16})$$

where the fourth central moment is given by:

$$m_{ijkl} = \chi_{ijkl} + \chi_{ij}\chi_{kl} + \chi_{ik}\chi_{jl} + \chi_{il}\chi_{jk}. \quad (\text{S17})$$

Therefore, the exact equations of motion are:

$$\begin{aligned} \dot{\chi}_i &= \sum_k s_k \chi_{ik} + \sum_{k < l} s_{kl} (\chi_{ikl} + \chi_{ik}\chi_l + \chi_k\chi_{il}) & , \\ \dot{\chi}_{ij} &= \sum_k s_k \chi_{ijk} + \sum_{k < l} s_{kl} (\chi_{ijkl} + \chi_{ik}\chi_{jl} + \chi_{il}\chi_{jk} + \chi_{ijk}\chi_l + \chi_k\chi_{ijl}) & . \end{aligned} \quad (\text{S18})$$

exQLE calculation

As the following calculations are valid for both the Gibbs distribution, and the cumulant distribution of any arbitrary distribution after taking the limit of $\phi \rightarrow 0$, we assume that the genotype distribution takes the form of a Gibbs distribution for simplicity. For further simplicity, we drop ϕ from χ_i^ϕ , χ_{ij}^ϕ , and also omit the operation of taking the limit as $\phi \rightarrow 0$. The equation of motion for the first-order cumulant is straightforward to obtain (Eq. (5) in Main), using the relationships $\partial_{\phi_i} \chi_k = \chi_{ik}$ and $\partial_{\phi_i} \chi_{kl} = \chi_{ikl}$, which arise from the properties of the cumulant generating function or the normalization of the Gibbs distribution.

Here, we focus on the equation of motion for the second-order cumulant. The direct calculation of the exQLE for the second-order cumulants yields Eq. (6) in Main, which is given as:

$$\begin{aligned} \partial_{\phi_i} \partial_{\phi_j} \langle F \rangle &= \partial_{\phi_j} \left(\sum_k (\partial_{\phi_i} \chi_k) \partial_{\chi_k} \langle F \rangle + \sum_{k < l} (\partial_{\phi_i} \chi_{kl}) \partial_{\chi_{kl}} \langle F \rangle \right) \\ &= \sum_k (\partial_{\phi_j} \partial_{\phi_i} \chi_k) \partial_{\chi_k} \langle F \rangle + \sum_{k < l} (\partial_{\phi_j} \partial_{\phi_i} \chi_{kl}) \partial_{\chi_{kl}} \langle F \rangle + \sum_k (\partial_{\phi_i} \chi_k) \partial_{\phi_j} \partial_{\chi_k} \langle F \rangle + \sum_{k < l} (\partial_{\phi_i} \chi_{kl}) \partial_{\phi_j} \partial_{\chi_{kl}} \langle F \rangle^0 \\ &= \sum_k \chi_{ijk} \partial_{\chi_k} \langle F \rangle + \sum_{k < l} \chi_{ijkl} \partial_{\chi_{kl}} \langle F \rangle + \sum_k \chi_{ik} \left(\sum_l \chi_{jl} \partial_{\chi_l} \partial_{\chi_k} \langle F \rangle + \sum_{l < m} \chi_{jlm} \partial_{\chi_{lm}} \partial_{\chi_k} \langle F \rangle \right)^0 \\ &= \sum_k \chi_{ijk} \partial_{\chi_k} \langle F \rangle + \sum_{k < l} (\chi_{ijkl} + \chi_{ik}\chi_{jl} + \chi_{il}\chi_{jk}) \partial_{\chi_{kl}} \langle F \rangle & . \end{aligned} \quad (\text{S19})$$

Here, we used the fact that the derivative of the average fitness beyond the second-order cumulant vanishes. Additionally we used: $\partial_{\chi_k} \partial_{\chi_l} \langle F \rangle = \partial_{\chi_{kl}} \langle F \rangle$ and

$$\sum_{k,l} \chi_{ik}\chi_{jl} \partial_{\chi_{kl}} \langle F \rangle = \sum_{k < l} (\chi_{ik}\chi_{jl} + \chi_{il}\chi_{jk}) \partial_{\chi_{kl}} \langle F \rangle. \quad (\text{S20})$$

The equations of motion for exQLE (Eq. (8)-(9) in Main) lead to:

$$\begin{aligned} \dot{\chi}_i &= \sum_k \chi_{ik} \partial_{\chi_k} \langle F \rangle + \sum_{k < l} \chi_{ikl} \partial_{\chi_{kl}} \langle F \rangle \\ &= \sum_k \chi_{ik} \left(s_k + \sum_{l;l>k} s_{kl} \chi_l + \sum_{l;l<k} s_{lk} \chi_l \right) + \sum_{k < l} s_{kl} \chi_{ikl} \\ &= \sum_k \chi_{ik} s_k + \sum_{k < l} s_{kl} (\chi_{ik}\chi_l + \chi_{il}\chi_k + \chi_{ikl}) & , \end{aligned} \quad (\text{S21})$$

and

$$\begin{aligned}
\dot{\chi}_{ij} &= \sum_k \chi_{ijk} \partial_{\chi_k} \langle F \rangle + \sum_{k < l} (\chi_{ijkl} + \chi_{ik}\chi_{jl} + \chi_{il}\chi_{jk}) \partial_{\chi_{kl}} \langle F \rangle \\
&= \sum_k \chi_{ijk} \left(s_k + \sum_{l;l>k} s_{kl}\chi_l + \sum_{l;l<k} s_{lk}\chi_l \right) + \sum_{k < l} s_{kl}(\chi_{ijkl} + \chi_{ik}\chi_{jl} + \chi_{il}\chi_{jk}) \\
&= \sum_k s_k \chi_{ijk} + \sum_{k < l} s_{kl}(\chi_{ijk}\chi_l + \chi_{ijl}\chi_k + \chi_{ijkl} + \chi_{ik}\chi_{jl} + \chi_{il}\chi_{jk}) .
\end{aligned} \tag{S22}$$

Here, where we used:

$$\sum_k \chi_{ik} \sum_{l;l < k} s_{lk}\chi_l = \sum_{k < l} s_{kl}\chi_{il}\chi_k \tag{S23}$$

by simply renaming indices. The two sets of equations are identical.

Therefore, we directly confirmed that the equations of motion for the first and second cumulants, derived from the exact Price's equation and the exQLE equation, yield identical results in the case of pairwise fitness.

Proof of positive semidefiniteness of $D(\chi)$ matrix for $K \in \{1, 2\}$

For the $K = 1$ case, $D(\chi)$ is trivially positive semidefinite. For $K = 2$ case, by defining $\Delta_i := g_i - \chi_i$, it can be expressed as

$$\begin{aligned}
D(\chi) &= \begin{pmatrix} \chi_{ik} & \chi_{ikl} \\ \chi_{ijk} & \chi_{ijkl} + \chi_{ik}\chi_{jl} + \chi_{il}\chi_{jk} \end{pmatrix} \\
&= \left\langle \begin{pmatrix} \Delta_i \Delta_j & \Delta_i \Delta_k \Delta_l \\ \Delta_i \Delta_j \Delta_k & (\Delta_i \Delta_j - \chi_{ij})(\Delta_k \Delta_l - \chi_{kl}) \end{pmatrix} \right\rangle \\
&= \left\langle \begin{pmatrix} \Delta_i & \Delta_k \\ \Delta_i \Delta_j - \chi_{ij} & \Delta_k \Delta_l - \chi_{kl} \end{pmatrix}^\top \right\rangle \succeq 0 .
\end{aligned} \tag{S24}$$

From the second line to the third line, we used the fact $\langle \Delta_i \Delta_j \Delta_k \rangle = \langle (\Delta_i \Delta_j - \chi_{ij}) \Delta_k \rangle$. Therefore, $D(\chi)$ is positive semidefinite.

Derivation of the cumulant dynamics from genotype dynamics

We denote the genotype distribution $P(\mathbf{g})$ for $\mathbf{g} \in \{-1, 1\}^L$ as $P(\mathbf{g}^a) \mapsto z_a$, where each unique genotype is indexed by $a \in \{1, \dots, 2^L\}$. We also denote genotype-level selection coefficient as h_a , such that the fitness function satisfies $F(\mathbf{g}^a) = \bar{F} + h_a$. The average fitness is then given by

$$\langle F \rangle = \bar{F} + \sum_a h_a z_a = \bar{F} + \sum_{\mathcal{J}} s_{\mathcal{J}} \mu_{\mathcal{J}} . \tag{S25}$$

Here, $\mu_{\mathcal{J}}$ denote a moment indexed by the set \mathcal{J} (which may include multiple indices), and given by

$$\mu_{\mathcal{J}} = \sum_a z_a \prod_{j \in \mathcal{J}} g_j^a . \tag{S26}$$

Let define the matrix,

$$\mathcal{G}_{a,\mathcal{J}} = \prod_{j \in \mathcal{J}} g_j^a , \tag{S27}$$

so that the moments and genotype distributions are related via $\boldsymbol{\mu} = \mathcal{G}^\top \mathbf{z}$. Given Fisher's fundamental theorem, the genotype distribution evolves as

$$\dot{z}_a = \sum_{ab} C_{ab}(\mathbf{z}) h_b \tag{S28}$$

where

$$C_{ab}(\mathbf{z}) = z_a \delta_{a,b} - z_a z_b , \tag{S29}$$

is the covariance matrix of genotype frequencies. In the vector form, it can be expressed as $\dot{\mathbf{z}} = C(\mathbf{z})\mathbf{h} = C(\mathbf{z})\nabla_{\mathbf{z}}\langle F \rangle$. Since $\langle F \rangle$ depends on \mathbf{z} via the moments $\boldsymbol{\mu}$, we apply the chain rule:

$$\frac{\partial \langle F \rangle}{\partial z_a} = \sum_{\mathcal{J}} \frac{\partial \mu_{\mathcal{J}}}{\partial z_a} \frac{\partial \langle F \rangle}{\partial \mu_{\mathcal{J}}} = \sum_{\mathcal{J}} \mathcal{G}_{a,\mathcal{J}} \frac{\partial \langle F \rangle}{\partial \mu_{\mathcal{J}}} \quad , \quad (\text{S30})$$

which can be expressed in vector form $\nabla_{\mathbf{z}}\langle F \rangle = \mathcal{G}\nabla_{\boldsymbol{\mu}}\langle F \rangle$.

Substituting into the dynamics:

$$\dot{\mathbf{z}} = C(\mathbf{z})\mathcal{G}\nabla_{\boldsymbol{\mu}}\langle F \rangle \quad . \quad (\text{S31})$$

Using the relation $\boldsymbol{\mu} = \mathcal{G}^{\top}\mathbf{z}$, the moment dynamics become

$$\dot{\boldsymbol{\mu}} = \mathcal{G}^{\top}C(\mathbf{z})\mathcal{G}\nabla_{\boldsymbol{\mu}}\langle F \rangle \quad , \quad (\text{S32})$$

which can be further transformed by using the chain rule:

$$\dot{\boldsymbol{\mu}} = \mathcal{G}^{\top}C(\mathbf{z})\mathcal{G}\left(\nabla_{\boldsymbol{\mu}}\boldsymbol{\chi}^{\top}\right)\nabla_{\boldsymbol{\chi}}\langle F \rangle \quad . \quad (\text{S33})$$

Transforming from moments to cumulants using the Jacobian matrix: $d\boldsymbol{\mu} = (\nabla_{\boldsymbol{\chi}}\boldsymbol{\mu}^{\top})^{\top}d\boldsymbol{\chi}$. Substituting this into the dynamics gives: $\dot{\boldsymbol{\mu}} = (\nabla_{\boldsymbol{\chi}}\boldsymbol{\mu}^{\top})^{\top}\dot{\boldsymbol{\chi}}$.

By using the relation,

$$\left(\left(\nabla_{\boldsymbol{\chi}}\boldsymbol{\mu}^{\top}\right)^{\top}\right)^{-1} = \left(\left(\nabla_{\boldsymbol{\chi}}\boldsymbol{\mu}^{\top}\right)^{-1}\right)^{\top} = \left(\nabla_{\boldsymbol{\mu}}\boldsymbol{\chi}^{\top}\right)^{\top} \quad ,$$

we obtain the cumulant dynamics:

$$\dot{\boldsymbol{\chi}} = D(\boldsymbol{\chi})\nabla_{\boldsymbol{\chi}}\langle F \rangle \quad , \quad (\text{S34})$$

where

$$D(\boldsymbol{\chi}) = \left(\nabla_{\boldsymbol{\mu}}\boldsymbol{\chi}^{\top}\right)^{\top}\mathcal{G}^{\top}C(\mathbf{z})\mathcal{G}\left(\nabla_{\boldsymbol{\mu}}\boldsymbol{\chi}^{\top}\right) \quad . \quad (\text{S35})$$

This is the matrix $D(\boldsymbol{\chi})$ appearing in Eq. (7) of the main text. Its origin lies in $C(\mathbf{z})$, which arises from competition between genotypes and also serves as the covariance matrix in the diffusion process. Importantly, since $C(\mathbf{z})$ is symmetric and positive semidefinite, the matrix $D(\boldsymbol{\chi})$ inherits these properties, it is symmetric and positive semidefinite as well.

Derivation of the equation to infer fitness values

We now derive the equation used to infer fitness parameters from cumulant dynamics.

The cumulant dynamics described in Eq. (10) have been deterministic, assuming an infinitely large population. For a finite population of size N , however, stochastic effects must be considered. In this case, the dynamics become a Langevin equation:

$$\dot{\boldsymbol{\chi}} = D(\boldsymbol{\chi})\nabla_{\boldsymbol{\chi}}\langle F \rangle + \boldsymbol{\eta}(t) \quad , \quad (\text{S36})$$

where $\boldsymbol{\eta}(t)$ is a noise vector satisfying $\langle \boldsymbol{\eta}_{\mathcal{J}(t)}\boldsymbol{\eta}_{\mathcal{K}(t')} \rangle = D_{\mathcal{J},\mathcal{K}}(\boldsymbol{\chi}(t))\delta(t-t')$.

This Langevin equation is equivalent to the following Fokker–Planck equation⁸¹:

$$\partial_t P(\boldsymbol{\chi}, t) = -\nabla_{\boldsymbol{\chi}}^{\top}D(\boldsymbol{\chi})\nabla_{\boldsymbol{\chi}}\langle F \rangle P(\boldsymbol{\chi}, t) + \frac{N}{2}\text{Tr}\left(\nabla_{\boldsymbol{\chi}}\nabla_{\boldsymbol{\chi}}^{\top}D(\boldsymbol{\chi})\right)P(\boldsymbol{\chi}, t) \quad . \quad (\text{S37})$$

The Fokker–Planck equation can be rewritten as a probability density over entire cumulant trajectories. For numerical implementation, we discretize time at points t_k for $k \in \{0, 1, \dots, K+1\}$, and define $\Delta t_k := t_{k+1} - t_k$ and $\Delta\boldsymbol{\chi}(t_k) := \boldsymbol{\chi}(t_{k+1}) - \boldsymbol{\chi}(t_k)$.

The probability of a cumulant trajectory is then expressed as

$$P((\boldsymbol{\chi}(t_k))_{k=0}^{K+1}) \propto e^{-N\mathcal{S}((\boldsymbol{\chi}(t_k))_{k=0}^{K+1})} \quad , \quad (\text{S38})$$

where \mathcal{S} is given by

$$\begin{aligned} \mathcal{S}((\boldsymbol{\chi}(t_k))_{k=0}^{K+1}) &= \sum_{k=0}^K \frac{1}{2\Delta t_k} \left[\Delta\boldsymbol{\chi}(t_k) - \Delta t_k D(\boldsymbol{\chi}(t_k))\nabla_{\boldsymbol{\chi}}\langle F \rangle \right]^{\top} \\ &\quad \times D^{-1}(\boldsymbol{\chi}(t_k)) \left[\Delta\boldsymbol{\chi}(t_k) - \Delta t_k D(\boldsymbol{\chi}(t_k))\nabla_{\boldsymbol{\chi}}\langle F \rangle \right] \quad , \end{aligned} \quad (\text{S39})$$

Since \mathcal{S} is quadratic in $\nabla_{\chi} \langle F \rangle$, the maximum likelihood estimate of the fitness parameters can be obtained analytically by solving the following linear equation:

$$\sum_{k=0}^K \Delta \chi(t_k) = \sum_{k=0}^K \Delta t_k D(\chi(t_k)) \nabla_{\chi} \langle F \rangle \quad . \quad (\text{S40})$$

By solving the above maximum likelihood equation, which is linear in s , we can obtain s .

Efficient computation of the forward exQLE simulation under higher-order fitness

To obtain cumulant dynamics using either the exQLE framework or the exQLE with a Gaussian closure scheme, we must evaluate the products of the diffusion matrix, which involve third and fourth-order cumulants and fitness parameters. However, a direct computation of the diffusion matrix and its product with fitness parameters is computationally expensive. Estimating these values across multiple time points, on the order of 100 different time points, requires significant computational time. Additionally, incorporating a fitness function that depends on four-way interactions further increases computational complexity. To improve computational efficiency, we outline an optimized approach for computing cumulant dynamics.

Denote the gradient of the average fitness, which serves as the effective fitness parameter vector consisting of selection and epistatic coefficients, as $\begin{pmatrix} \hat{s}_k \\ \hat{s}_{kl} \end{pmatrix} := \begin{pmatrix} \partial_{\chi_k} \\ \partial_{\chi_{kl}} \end{pmatrix} \langle F \rangle$. For the fitness function with four-way interactions, let μ_i, μ_{ij}, \dots denote mutation frequencies, and let $\langle F \rangle = \bar{F} + \sum_i s_i \mu_i + \sum_{i < j} s_{ij} \mu_{ij} + \sum_{i < j < k} s_{ijk} \mu_{ijk} + \sum_{i < j < k < l} s_{ijkl} \mu_{ijkl}$ represent the effective fitness parameters as

$$\begin{pmatrix} \hat{s}_k \\ \hat{s}_{kl} \end{pmatrix} = \begin{pmatrix} s_k + \sum_{i < k} s_{ik} \mu_i + \sum_{i < j; i < k} s_{ijk} \mu_{ij} + \sum_{i < j < l; i < k} s_{ijkl} \mu_{ijl} \\ s_{kl} + \sum_{i; i < k < l} s_{ikl} \mu_i + \sum_{i < j; i < k < l} s_{ijkl} \mu_{ij} \end{pmatrix} \quad . \quad (\text{S41})$$

These products between fitness parameters and moments can be computed as the sum of matrix-vector products, $s_{ijk} \mu_{ij} = \sum_{i < j (< k)} \langle s_{ijk} g_i g_j \rangle$ and $s_{ijkl} \mu_{ijl} = \sum_{i < j < l (< k)} \langle s_{ijkl} g_i g_j g_l \rangle$.

Let $\Delta_i := g_i - \chi_i$, then the cumulants can be obtained by $\chi_i = \langle \Delta_i \rangle, \chi_{ij} = \langle \Delta_i \Delta_j \rangle, \chi_{ijk} = \langle \Delta_i \Delta_j \Delta_k \rangle, \chi_{ijkl} = \langle \Delta_i \Delta_j \Delta_k \Delta_l \rangle - (\chi_{ik} \chi_{jl} + \chi_{il} \chi_{jk} + \chi_{ij} \chi_{kl})$. Additionally, define $\chi^{(2)}$ as the second-order cumulant in matrix form and \hat{S} as the effective epistasis matrix, where \hat{s}_{kl} occupies the k -th row and l -th column. Thus, the cumulant dynamics can be expressed in the following computationally more efficient form:

$$\begin{pmatrix} \dot{\chi}_i \\ \dot{\chi}_{ij} \end{pmatrix} = \begin{pmatrix} \chi_{ik} & \chi_{ikl} \\ \chi_{ijk} & \chi_{ijkl} + \chi_{ik} \chi_{jl} + \chi_{il} \chi_{jk} \end{pmatrix} \begin{pmatrix} \hat{s}_k \\ \hat{s}_{kl} \end{pmatrix} = \begin{pmatrix} \langle \delta(\Delta^\top \hat{s}) \rangle + \langle \Delta(\Delta^\top \hat{S} \Delta) \rangle / 2 \\ \langle \Delta \Delta^\top (\Delta^\top \hat{s}) \rangle + \langle \Delta \Delta^\top \Delta^\top \hat{S} \Delta \rangle - \chi^{(2)} \text{Sum}(\chi^{(2)} \odot \hat{S}) \end{pmatrix}. \quad (\text{S42})$$

The last expression in Eq. (S42) is efficient because this computation never explicitly requires obtaining matrices or matrix products with more than $\mathcal{O}(L^2)$ elements.

For the Gaussian closure scheme, the cumulant dynamics can be obtained in the same manner. The dynamics under the Gaussian closure scheme are given by:

$$\begin{aligned} \begin{pmatrix} \dot{\chi}_i \\ \dot{\chi}_{ij} \end{pmatrix} &= \begin{pmatrix} \chi_{ik} & \chi_{ikl}(\delta_{ik} + \delta_{jk}) \\ \chi_{ijk}(\delta_{ik} + \delta_{jk}) & \chi_{ijkl}\delta_{ik}\delta_{jl} + \chi_{ik}\chi_{jl} + \chi_{il}\chi_{jk} \end{pmatrix} \begin{pmatrix} \hat{s}_k \\ \hat{s}_{kl} \end{pmatrix} \\ &= \begin{pmatrix} \chi_{ik} & \chi_{ikl}(\delta_{ik} + \delta_{jk}) \\ \chi_{ijk}(\delta_{ik} + \delta_{jk}) & [\langle \Delta_i \Delta_j \Delta_i \Delta_j \rangle - \chi_{ii} \chi_{jj} - 2\chi_{ij}^2] \delta_{ik} \delta_{jl} + \chi_{ik} \chi_{jl} + \chi_{il} \chi_{jk} \end{pmatrix} \begin{pmatrix} \hat{s}_k \\ \hat{s}_{kl} \end{pmatrix} \\ &= \begin{pmatrix} \langle \Delta(\Delta^\top \hat{s}) \rangle + \left\langle \Delta \odot \left(\sum_k \left\{ (\Delta \Delta^\top \odot \hat{S})_{ik} + (\Delta \Delta^\top \odot \hat{S})_{ki} \right\} \right)_{i=1}^L \right\rangle \\ \left\langle \Delta \Delta^\top \odot (\mathbf{1}(\Delta \odot \hat{s})^\top + (\Delta \odot \hat{s}) \mathbf{1}^\top) \right\rangle + \text{diag} \left(\left((\langle \Delta_i^2 \Delta_j^2 \rangle - \chi_{ii} \chi_{jj} - 2\chi_{ij}^2) s_{ij} \right)_{i < j} \right) + \chi^{(2)} \hat{S} \chi^{(2)} \end{pmatrix}, \end{aligned} \quad (\text{S43})$$

where $\mathbf{1}$ is a vector of length L consisting entirely of ones, \odot denotes the elementwise product, and the notation $(a_i)_i^L = (a_1, \dots, a_L)^\top$ is used.

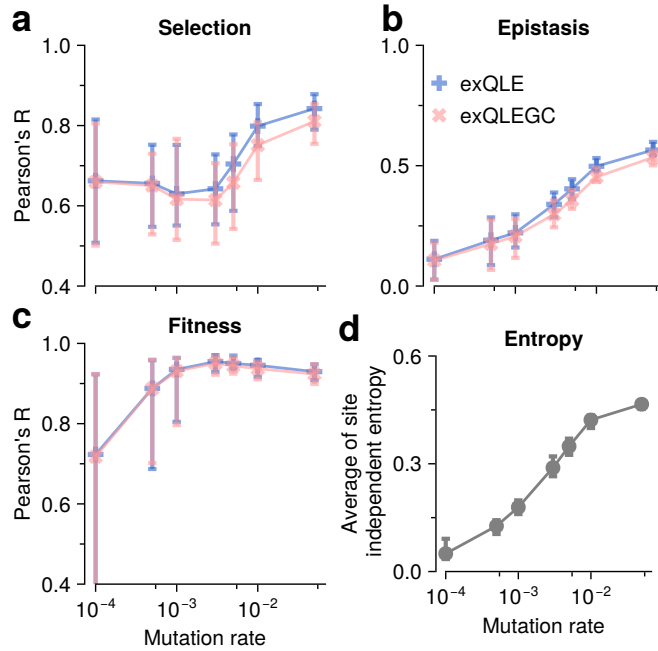


Fig. S1. Accuracy of inferred fitness parameters under higher-order fitness function. This corresponds to **Fig. 2** in the main text, but here the underlying selective pressure is determined by a higher-order fitness function rather than a pairwise one, that is, $K^* = 4$, where K^* denotes the highest order of cumulants in the averaged fitness function (as defined in the main text). The functionality and model parameters are the same as those used in the simulation for **Fig. 1**. The inference approach remains pairwise ($K = 2$), aiming to infer additive (selection) and pairwise (epistatic) fitness parameters. Despite the increased complexity of the true fitness landscape, the inferred parameters show high accuracy, as measured by Pearson's R values, for selection, epistasis, and overall fitness. The dependency of accuracy on mutation rate remains qualitatively similar to that observed under the pairwise fitness setting.

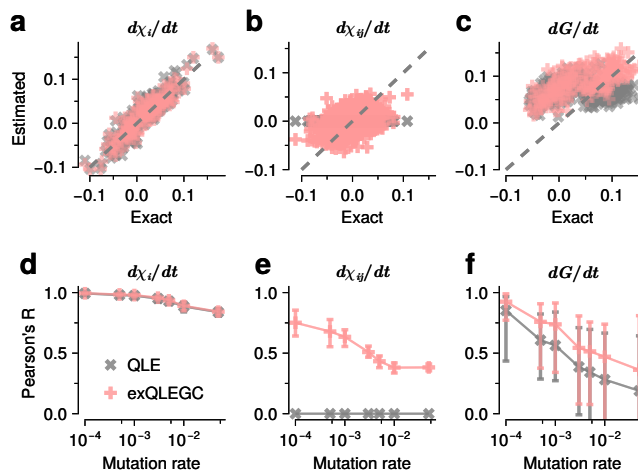


Fig. S2. Dynamics of cumulants and traits using exQLE and Gaussian closure scheme. This corresponds to **Fig. 1** in the main text but utilizes the exQLE framework with a Gaussian closure (GC) scheme, which suppresses all cumulants beyond second order. The GC scheme is efficient for inferring fitness parameters and is not limited to inference problems; it is also applicable to forward processes. Although the accuracy of the dynamics for cumulants (b) is not as high as that in the exQLE case without GC, the estimated values show a reasonable correlation with those from the exact calculations. Pearson's R values for additive selection (a), pairwise epistasis (b), and random traits (c) for exQLE with GC are 0.93, 0.43, and 0.65. For comparison, the exQLE values without GC are 0.97, 0.89, and 0.95, respectively.

Supplementary References

78. Neher, R. A. & Shraiman, B. I. Statistical genetics and evolution of quantitative traits. *Reviews of Modern Physics* **83**, 1283 (2011).
79. Zeng, H.-L. & Aurell, E. Inferring genetic fitness from genomic data. *Physical Review E* **101**, 052409 (2020).
80. Wright, S. Evolution in mendelian populations. *Genetics* **16**, 97 (1931).

81. Risken, H. Fokker-planck equation. In *The Fokker-Planck equation: methods of solution and applications*, 63–95 (Springer, 1989).